Jahn-Teller assisted polaron hopping and associated dielectric response of PrFe0.5Mn0.5O2.95

C. Ganeshraj, S. Kavita, R. Mahendiran, Neetika Sharma, A. Das et al.

Citation: Appl. Phys. Lett. **103**, 112909 (2013); doi: 10.1063/1.4821190
View online: http://dx.doi.org/10.1063/1.4821190
View Table of Contents: http://apl.aip.org/resource/1/APPLAB/v103/i11
Published by the AIP Publishing LLC.

Jahn-Teller assisted polaron hopping and associated dielectric response of $PrFe_{0.5}Mn_{0.5}O_{2.95}$

C. Ganeshraj,[1] S. Kavita,[2] R. Mahendiran,[2] Neetika Sharma,[3] A. Das,[3] and P. N. Santhosh[1,a)]
[1]*Low Temperature Physics Laboratory, Department of Physics, Indian Institute of Technology Madras, Chennai 600 036, India*
[2]*Department of Physics, Faculty of Science, National University of Singapore, 2 Science Drive 3, Singapore*
[3]*Solid State Physics Division, Bhabha Atomic Research Centre, Mumbai 400 085, India*

(Received 20 May 2013; accepted 29 August 2013; published online 13 September 2013)

The canted G-type antiferromagnet $PrFe_{0.5}Mn_{0.5}O_{2.95}$ shows an enhanced Jahn-Teller (JT) distortion below 150 K (T*). The resistivity of the grains can be described by variable range hopping between the localized states, and there is a dominant grain boundary contribution to dc resistivity, below T*. Above T^*, the total dc resistivity follows small polaron hopping (SPH) conduction. A giant dielectric response is observed, and it can be ascribed to Maxwell-Wagner polarization and SPH mechanism. Despite the low concentration of JT active Mn^{3+} ions, our result indicates an important role of JT effect on physical properties of $PrFe_{0.5}Mn_{0.5}O_{2.95}$. © *2013 AIP Publishing LLC*. [http://dx.doi.org/10.1063/1.4821190]

Over past few years, materials exhibiting a colossal dielectric constant (CDC), $\varepsilon' > 10^3$, have gained a great attention due to their application in memory devices based on capacitive elements.[1] Many transition-metal oxides show very high magnitude of dielectric constant and have immense potential applications in the development of new capacitance-based energy storage devices. Among the various perovskite oxides, $DyMnO_3$ and Sr_2TiMnO_6, colossal dielectric constant has been realized through hopping charge transport and Maxwell-Wagner (MW) effect.[2,3]

$PrFeO_3$ exhibits colossal dielectric constant with $\varepsilon' \sim 10^4$ (Ref. 4) and also has G-type antiferromagnetic structure with $T_N = 707$ K.[5] In $PrFeO_3$, Fe^{3+} is orbitally non-degenerate and the distortion in the FeO_6 octahedra is driven entirely by the ionic-size effect,[6] whereas in $PrMnO_3$, Mn^{3+} is a Jahn-Teller (JT) ion and the distortion in MnO_6 is due to JT distortion and octahedra tilting. In $PrMnO_3$, a small canting below Néel temperature ($T_N = 99$ K) arises from the canting of the A-type antiferromagnetic (AFM) structure due to Dzyaloshinskii-Moriya (DM) interaction, which is generated by a buckling of the orthorhombic oxygen octahedra. Moreover, in $REMnO_3$ (RE = La, Pr, Dy, Ho,…), the splitting of Mn 3*d* states due to crystal field effects leads to an e_g doublet and t_{2g} triplet, and this degeneracy usually lifted by orbital–lattice interaction is known as cooperative JT effect. The coupling between JT phonons and e_g electrons could make the carriers localized and even generate related polarons. Since the ionic radii and charge of Fe^{3+} and Mn^{3+} are similar, doping Mn^{3+} for Fe^{3+} in $PrFeO_3$ will bring disorder in the system, and it will also lead to different magnetic ordering temperatures of the transition metal ions Fe^{3+} and Mn^{3+} through various kinds of magnetic interactions (such as Fe^{3+}-O-Fe^{3+}, Fe^{3+}-O-Mn^{3+}, and Mn^{3+}-O-Mn^{3+}). One may expect ferroelectricity at these ordering temperatures, and its origin is attributed to disordered cations of non-equivalent spins at the B-sites and/or MW relaxation.[7] Along with JT effect from Mn^{3+} ions, the disorder also leads to localization, and charge carriers hopping between these localized states are also responsible for conductivity.

In this study, we present temperature dependent neutron diffraction studies, electrical resistivity, and impedance spectroscopy of polycrystalline $PrFe_{0.5}Mn_{0.5}O_{2.95}$ (PFMO). A quantitative analysis of dielectric relaxation and localized charge carriers migration behaviour over a temperature range of 100 K to 300 K is performed. A possible correlation between JT distortions and the behaviour of hopping conduction has been identified, through neutron diffraction results.

PFMO sample was prepared by solid state reaction.[8] Neutron diffraction data were recorded on a multi position sensitive detector (PSD) based powder diffractometer ($\lambda = 1.2443$ Å) at Dhruva reactor, Bhabha Atomic Research Centre, Mumbai. Rietveld refinement of the neutron diffraction patterns were carried out using FULLPROF program.[9] Dielectric characteristics and dc conductivity were studied using Janis optical cryostat with Agilent 4294A Precision LCR meter and Keithley 617 electrometer, respectively. Differential scanning calorimetry (DSC) measurements were made on a Netzsch DSC 204 F1 Phoenix with the heating rate of 20 K/min.

Rietveld refinement of the neutron diffraction data of PFMO from 300 K to 5 K indicates that PFMO has orthorhombic structure (*Pnma*) with spin structure as Γ_2: C_x G_y F_z, in Bertaut's notation,[9] which has a net ferromagnetic moment along z–direction, and the spin component along x-direction (C_x) is found to be negligibly small. The typical refinement pattern and detailed information of refinement for PFMO at 300 K and 5 K are available online (see Figures 1(a) and 1(b) in supplementary material).[10] Canted antiferromagnetic behaviour can arise due to DM interaction as well as single ion anisotropy.[11,12] The observed oxygen non-stoichiometry in PFMO is ~0.05. Since PFMO was annealed at high temperature, the oxygen vacancies in PFMO are inevitable due to the lack of absorption during cooling process after annealing the sample,[13] leading to heterovalent Mn/Fe ions to keep the system electrically neutral.

a)santhosh@physics.iitm.ac.in. Tel.: +91 44 2257 4882. FAX: +91 44 2257 4852.

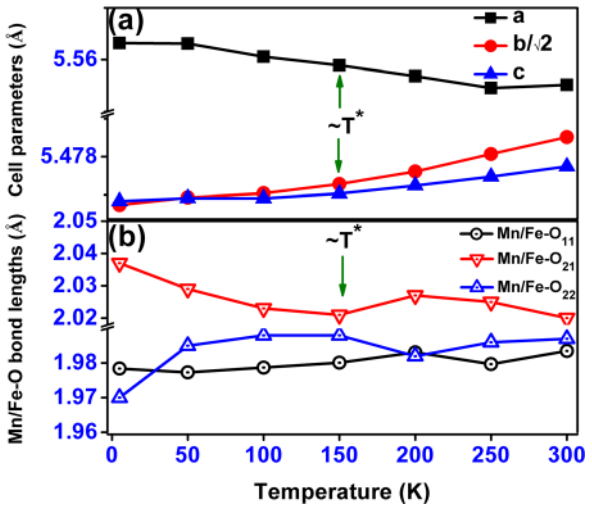

FIG. 1. Temperature variation of (a) lattice parameters and (b) Mn/Fe-O bond lengths. The solid lines are guides to the eye.

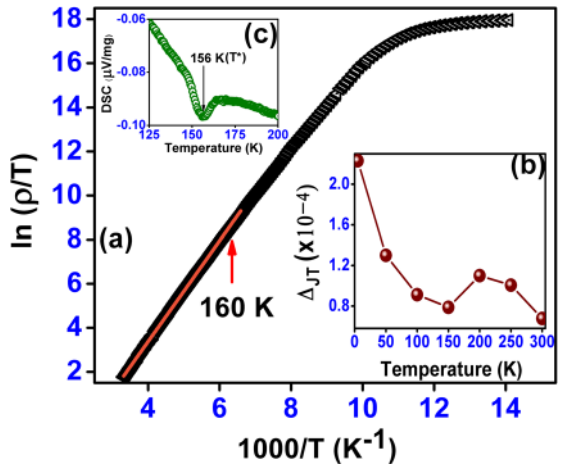

FIG. 2. (a) Plot of ln (ρ/T) vs. 1000/T for PFMO. (b) Temperature variation of JT distortion (Δ_{JT}) of PFMO. (c) DSC scan heating at 20 K min^{-1}.

Figure 1(a) shows the temperature variation of lattice parameters of PFMO. On lowering temperature, the observed expansion of lattice parameter "a" and contraction of "b" are attributed to JT distortion and octahedral tilting ($GdFeO_3$ type tilting),[14] whereas steady decrease in c indicates enhancement of the octahedral tilting distortion.[15] Figure 1(b) exhibits the temperature variation of Mn/Fe-O bond lengths in the Mn/Fe-O octahedra. The long (Mn/Fe-O_{21}) and medium (Mn/Fe-O_{22}) bond lengths of Mn/Fe-O bonds are predominantly in the ac plane, whereas the short (Mn-O_{11}) bond length of Mn/Fe-O bonds are along b-axis. While lowering temperature, the apical Mn/Fe–O_{11} bond length shows almost linear temperature dependence, whereas the equatorial Mn/Fe-O bond lengths diverge below room temperature and converge around 150 K, then again it diverges below 150 K, as shown in Figure 1(b), indicating the variation of octahedral distortion in the equatorial (ac) plane with temperature. The relative difference between apical and equatorial Mn/Fe–O bond lengths gives an indication of the possible octahedral JT distortion and its evolution with temperature. In order to understand the local structural change, the magnitude of JT distortion (Δ_{JT}) can be expressed as $\Delta_{JT} = \frac{1}{6}\sum_{n=1,6}[(d_n - \langle d\rangle)/\langle d\rangle)]^2$, where d_n (d) is the individual (average) Mn/Fe–O bond length shown in Figure 2(b).[16] The value of Δ_{JT} is small compared to that of $PrMnO_3$[17] (43.1×10^{-4}) and is close to that of $Y_{0.15}Ca_{0.85}MnO_3$[16] owing to the low concentration of JT active Mn^{3+} ions. Around 150 K (T^*), there is an anomalous change of slope, and below 150 K, Δ_{JT} is slightly enhanced in PFMO. Moreover, a change in slope is observed in the temperature variation of the lattice parameters of PFMO around T^* as shown in Figure 1(a).

Above 160 K, the electrical resistivity data of PFMO could be fitted very well with small polaron hopping (SPH) model (Figure 2(a)), $\rho/T = \rho_\alpha \exp(E_p/k_BT)$, where ρ_α is the pre-exponential factor, k_B is the Boltzmann constant, and $E_p = W_H + W_D/2$ is the activation energy, W_H and W_D are hopping and disorder energies. The estimated activation energy is ~0.20 eV and the plot acquires curvature towards higher resistivity below 160 K. The activation energy is similar to those found in materials in which electronic transport occurs by means of hopping between localized states as a consequence of the formation of small polaron, which contains oxygen vacancies and/or JT type electron-phonon interactions.[18,19] The deviation from small polaron model fit (Figure 2(a)) indicates that a different kind of conduction occurs below and above 160 K.

Since JT distortion shows an anomalous behaviour around T^* and resistivity data show a deviation from SPH around 160 K, DSC has been performed. An exothermic peak is observed at 156 K (Figure 2(c)) during heating process, close to the anomaly found in neutron diffraction and resistivity data.

Figures 3(a) and 3(b) (and 3(c)) show the temperature dependence of the dielectric constant ε' (with $\varepsilon' > 10^4$ at 300 K)

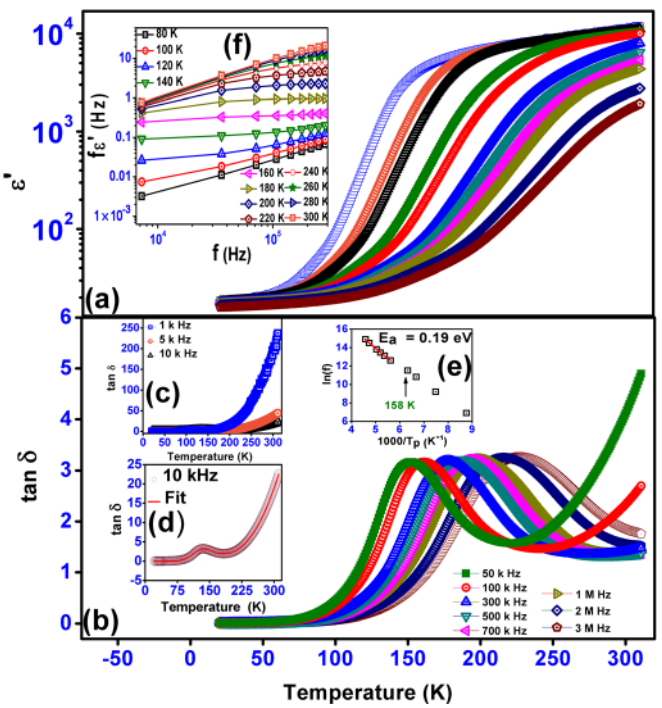

FIG. 3. Temperature dependence of (a) ε' at various frequencies, (b) tan δ at various frequencies, (c) tan δ at three lowest frequencies (1 kHz, 5 kHz, and 10 kHz). (d) Least squares fitting of the experimental data at 10 kHz with help of Gaussian peak and an exponential background. (e) Arrhenius plot of tan δ relaxation frequency (the solid curves through data points are the fitting results). (f) Plot of log ($f\varepsilon'$) against log (f) for PFMO at number of fixed temperatures.

and tan δ (tan δ for three lowest frequencies) with frequencies, respectively. These curves indicate relaxor-like behaviour. ε' shows a high temperature plateau followed by a rapid drop when cooling through a critical temperature and has one plateau at the lower temperature. A relaxation peak in tan δ corresponding to the drop of ε' is observed.[20] Both the tan δ peak position and ε' drop temperature shift to higher temperature with increasing frequency, indicating a thermally activated behaviour. The exponential increasing background in tan δ (or in ε'') indicates that the background is associated with the hopping conductivity ($\varepsilon'' \sim \sigma/\omega$, where σ is conductivity and $\omega = 2\pi f$ is the angular frequency and for small polaron hopping $\sigma T = \sigma_\alpha \exp(-E_p/k_B T)$, where σ_α is the pre-exponential factor). In order to extract the peak position in temperature dependence of tan δ, a Gaussian peak superimposed on an exponential increasing background in a form of a + $be^{(-c/T)}$, with a, b, and c as adjustable parameters, was used for fitting. The least-square fit for 10 kHz is presented as solid curve, as a representative example, in Figure 3(d). Good agreement between experimental data and fitting is achieved. According to the thermally activated relaxation, above 158 K ($\sim T^*$), Arrhenius law is adopted to describe the relationship between the measuring frequency and peak temperature T_p (Figure 3(e)), as $f = f_o \exp(-E_a/k_B T)$, where f_0 is a pre-exponential factor and E_a is the activation energy. The estimated activation energy E_a is $\sim$0.19 eV. The closeness of the values of E_p and E_a may imply the similar origin corresponding to dc and ac conductivities, viz., similar localized charged carriers and hopping process. A distinct deviation from Arrhenius plot of ln f vs. $1/T_p$ at low temperatures (<158 K) indicates that different kind of conduction occurs below and above 158 K. This strongly suggests that the dielectric relaxation might originate from hopping conduction. In fact, the localized charge carriers hopping between spatially fluctuating lattice potentials not only produce conductivity but also give dipolar effects.[21] On the other hand, the frequency dependence of the dielectric behaviour of this kind of relaxation can be described by Jonscher's power law or universal dielectric response (UDR),[22] $f\varepsilon' = \tan(s\pi/2)\sigma_0/\varepsilon_0 f^s$, where σ_0 and s are temperature dependent constants and ε_0 is the electric permittivity of free space. For a given temperature, a straight line plot with slope s must be obtained in the plot of log ($f\varepsilon'$) vs. log f, and it is confirmed on the log–log graph in figure 3(f) wherein good straight lines are observed at high temperatures. While decreasing temperature, a gradual deviation from straight line behaviour occurs due to the freezing of charge carriers which reduce the dipolar effects.[21] Simultaneously, the freezing process increases the resistivity. These frozen carriers no longer contribute to the polarization and the observed dielectric behaviour is mainly due to the remaining charge carriers and it still obeys the UDR law. At lower temperatures, the freezing process moves out the measurable frequency range, the linear behaviour of log ($f\varepsilon'$) vs. log f appears again, as clearly shown in Figure 3(f). The UDR behaviour is known to be valid for semiconductors with hopping localized charge carriers.[21]

Figures 4(a) and 4(e) show typical complex impedance spectra of PFMO at 100 K and 300 K. The spectrum is resolved into two semicircles, and dielectric response could

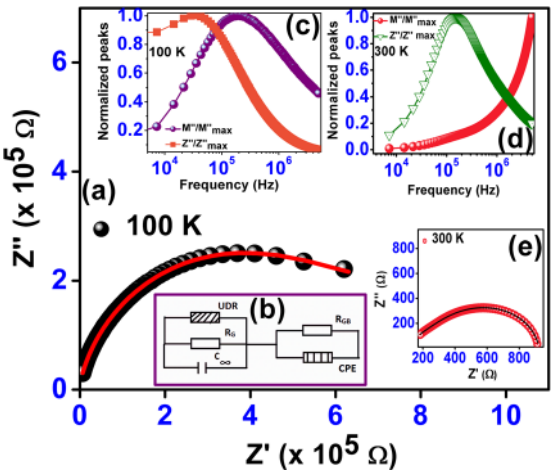

FIG. 4. (a) and (e) Nyquist diagram of complex impedance, (b) the equivalent circuit model, (c) and (d) are frequency variation of normalized impedance Z''/Z''_{max} and modulus M''/M''_{max} at 100 K and 300 K.

be assigned to the combined effect of grains (G) at high frequency and grain boundaries (GB) at low frequency. When an electric current passes through a compound which has inhomogeneous grain/grain boundary interfaces, because of the different electrical conductivities of two dielectric media, the charge carriers would be localized and accumulated at the interfaces under an external ac field. This process could give rise to MW interfacial relaxation.[22,23] The dielectric response is described by equivalent circuit model (ECM), as shown in Figure 4(b), which is in the frame of MW model and it is composed of series of two circuits, one with parallel GB resistance and a constant phase element and the other with parallel G resistance, capacitance, and UDR (indicative of conduction through polaron hopping). The ECM fit with the experimental data is in good agreement (Figures 4(a) and 4(e)) for 100 K and 300 K. The peaks of normalized impedance Z''/Z''_{max} and modulus M''/M''_{max} at 300 K do not coincide, but they nearly coincide at 100 K (Figures 4(d) and 4(c)). In general, a high resistance of GB and low capacitance of G results in a peak in the frequency variation of Z'' and M''.[24,25] Since the G and GB have different resistance and activation energies, their relaxation frequency will have different temperature dependence. So, normalized Z''/Z''_{max} and modulus M''/M''_{max} peaks will either diverge or converge with increasing or decreasing temperature. A dominant contribution from GB to the total dc resistivity was observed below T^*, whereas above T^*, a reduced contribution from GB with an increased contribution from G occurred, and around 300 K, nearly equal contribution from G and GB was observed. In order to check the underlying transport mechanism, the resistances of G and GB were extracted from the ECM fittings. At $T > T^*$, the resistivity data can be analyzed with small polaron nearest-neighbour hopping (NNH) with activation energy 0.15 and 0.18 eV for G and GB, respectively (Figure 5). These values support inhomogeneous character of the sample having low resistive G separated by more resistive GB.[26] At $T < T^*$, the resistivity of G was analyzed using variable range hopping (VRH) model, with ρ vs. T dependence $\rho = CT^{0.5} \exp(T_0/T)^{0.25}$, where C is a temperature-independent term and T_0 is a characteristic Mott temperature.[27–29] The slope of the ln ($\rho T^{-0.5}$) vs. $T^{-0.25}$

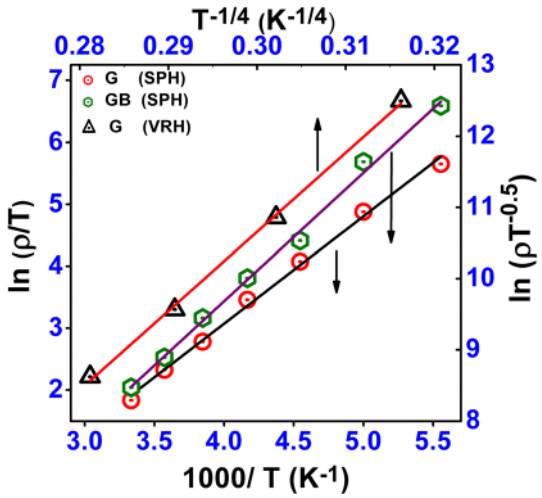

FIG. 5. Arrhenius plot of grain and grain boundary resistivity at $T > T^*$ and VRH plot of grain resistivity at $T < T^*$ obtained from the fittings of ECM.

curve (Figure 5) in the VRH conduction is used to determine T_o which is related to the density of states (DOS) $N(\varepsilon_F)$ at the Fermi level $T_0 = 21.2\alpha^3/N(\varepsilon_F)k_B$. By using an estimated value for the localization length $a = 1/\alpha$ (distance between two nearest neighbour Mn/Fe ions along b-axis, $a = 3.8707$ Å at 100 K) of electrons involved in hopping, the DOS at the Fermi level is $2.79 \times 10^{19}\,eV^{-1}\,cm^{-3}$ for G. The DOS value is of the order of $N(\varepsilon_F)$ in oxide semiconductors.[28] The dominant contribution from GB to dc resistivity and VRH in G below T^* leads to a deviation in dc resistivity from SPH below T^* (Figure 2(a)). The change of slope occurs in dc resistivity around 100 K, as shown in Figure 2(a), may be associated with the magnetic ordering of Mn ions.[7]

These results can be qualitatively explained within the framework of theoretical model of polaronic conduction. In the polaronic scenario,[27] at high temperatures, optical multiphonon process provides sufficient energy to polaron for hopping between nearest-neighbour localized states, resulting in SPH conduction. While decreasing temperature below T^*, as a consequence of disorder in a crystalline semiconductors/insulators, the hopping carriers are more localized due to Anderson localization.[30] Mott's VRH sets in G below T^* and the activation energy is essentially due to the disorder energy. Moreover, the localization of hopping carriers in G and dominant contribution from GB to dc resistivity leads a deviation from SPH conduction of dc resistivity below T^*.

Generally, a slow moving charge carrier induces lattice distortion, which acts as a potential well causing self-trapping of charge carrier. The quasiparticle formed by the charge carrier and its self-induced distortion, known as polaron, is originated from electron-phonon coupling and/or compositional/structural defects.[31–34] While decreasing temperature from room temperature, the JT distortion decreases slightly and then increases below T^*, indicating the polaron does not have enough activation energy below T^* for NNH due to localization and it follows VRH in G, along with a dominant contribution from GB to dc resistivity that leads to a deviation of dc resistivity from SPH conduction. Since the electron-phonon coupling mediated by JT distortion shows an anomalous behaviour around T^*, it may be the main origin of the formation of polarons. Moreover, the carriers hopping between heterovalent Mn/Fe ions formed by oxygen vacancies with different ionic radius may induce lattice deformation and thus also leading to the formation of polarons.[35,36]

In summary, $PrFe_{0.5}Mn_{0.5}O_{2.95}$ exhibits canted G-type antiferromagnetic ordering. The high resistivity below T^* is due to Anderson localization of polaronic charge carriers, ascribed to disorder in the compound, and a dominant contribution from GB to total resistivity. The giant dielectric behaviour of the compound arising from the MW polarization originates from grains and grain boundary interfaces and is governed by small polaron NNH conduction. The origin of the formation of polaron is mainly the JT distortion and also a contribution from lattice distortion induced by heterovalent Fe/Mn ions.

We thank Dr. R. Nirmala for her valuable suggestions. P.N.S. acknowledges Department of Science and Technology, India for financial assistance [Multiferroics project (SR/S2/CMP-25/2005)]. We thank Bhabha Atomic Research Centre for Neutron diffraction experiment.

[1]C. C. Homes, T. Vogt, S. M. Shapiro, S. Wakimoto, and A. P. Ramirez, Science **293**, 673 (2001).
[2]Y. Jang, J. He, J. Y. Zhu, W. Bai, L. Sun, X. J. Meng, X. D. Tang, C.-G. Duan, D. Rèmiens, J. H. Qiu, and J. H. Chu, Appl. Phys. Lett. **101**, 222904 (2012).
[3]K. R. S. Preethi Meher, M. Savinov, S. Kamba, V. Goian, and K. B. R. Varma, J. Appl. Phys. **108**, 094108 (2010).
[4]B. V. Prasad, G. Narsinga Rao, J. W. Chen, and D. Suresh babu, Solid State Sci. **14**, 225 (2012).
[5]J. Ma, J.-Q. Yan, S. O. Diallo, R. Stevens, A. Llobet, F. Trouw, D. L. Abernathy, M. B. Stone, and R. J. McQueeney, Phys. Rev. B **84**, 224115 (2011).
[6]D. Sånchez, J. A. Alonso, and M. J. Martínez-Lope, J. Chem. Soc. Dalton Trans. **2002**, 4422.
[7]B. Rajeswaran, P. Mandal, R. Saha, E. Suard, A. Sundaresan, and C. N. R. Rao, Chem. Mater. **24**, 3591 (2012).
[8]C. Ganeshraj, R. N. Mahato, D. Divyaa, and P. N. Santhosh, J. Appl. Phys. **107**, 09E305 (2010).
[9]G. T. Rado and H. Suhl, *Magnetism* (Academic Press, New York, 1963), Vol. III.
[10]See supplementary material at http://dx.doi.org/10.1063/1.4821190 for refined structural parameters of neutron diffraction data of $PrFe_{0.5}Mn_{0.5}O_{2.95}$ at 300 K and 5 K.
[11]I. Dzyaloshinsky, J. Phys. Chem. Solids **4**, 241 (1958).
[12]T. Moriya, Phys. Rev. **120**, 91 (1960).
[13]C. Ang, Z. Yu, Z. Jing, P. Lunkenheimer, and A. Loidl, Phys. Rev. B **61**, 3922 (2000).
[14]M. W. Lufaso and P. M. Woodward, Acta Crystallogr. **B60**, 10 (2004).
[15]P. M. Woodward, T. Vogt, D. E. Cox, A. Arulraj, C. N. R. Rao, P. Karen, and A. K. Cheetham, Chem. Mater. **10**, 3652 (1998).
[16]P. Tong, B. Kim, D. Kwon, B. G. Kim, G. Y. Ahn, J. M. S. Park, S. B. Kim, and S.-W. Cheong, Appl. Phys. Lett. **93**, 202504 (2008).
[17]J. A. Alonso, M. J. Martínez-Lope, M. T. Casis, and M. T. Fernåndez-Díaz, Inorg. Chem. **39**, 917 (2000).
[18]W. H. Jung, J. Phys.: Condens. Matter **10**, 8553 (1998).
[19]D. P. Karim and A. T. Aldred, Phys. Rev. B **20**, 2255 (1979).
[20]Z. Wang, X. M. Chen, L. Ni, and X. Q. Liu, Appl. Phys. Lett. **90**, 022904 (2007).
[21]C. C. Wang and L. W. Zhang, New J. Phys. **9**, 210 (2007).
[22]A. K. Jonscher, *Dielectric Relaxation in Solids* (Chelsea Dielectrics, London, 1983).
[23]P. Lunkenheimer, S. Krohns, S. Riegg, S. G. Ebbinghaus, A. Reller, and A. Loidl, Eur. Phys. J. Spec. Top. **180**, 61 (2009).
[24]R. Gerhardt, J. Phys. Chem. Solids **55**, 1491 (1994).
[25]J. Liu, C.-G. Duan, W.-G. Yin, W. N. Mei, R. W. Smith, and J. R. Hardy, Phys. Rev. B **70**, 144106 (2004).
[26]J. R. Macdonald, *Impedance Spectroscopy* (Wiley, New York, 1987).

[27]N. F. Mott and E. A. Davis, *Electronic Process in Non-Crystalline Materials* (Clarendon Press, Oxford, 1979).
[28]N. F. Mott, *Conduction in Non-Crystalline Materials* (Clarendon Press, Oxford, 1993).
[29]B. I. Shklovskii and A. L. Efros, *Electronic Properties of Doped Semiconductors* (Springer-Verlag, Berlin, 1984).
[30]A. P. Suotton, *Electronic Structure of Materials* (Clarendon Press, Oxford, 1993).
[31]K. K. Som and B. K. Chaudhuri, Phys. Rev. B **41**, 1581 (1990).
[32]I. G. Austin and N. F. Mott, Adv. Phys. **18**, 41 (1969).
[33]E. Iguchi, N. Kubota, T. Nakamori, N. Yamamoto, and K. J. Lee, Phys. Rev. B **43**, 8646 (1991).
[34]O. Bidault, M. Maglione, M. Actis, M. Kchikech, and B. Salce, Phys. Rev. B **52**, 4191 (1995).
[35]C. C. Wang, Y. M. Cui, and L. W. Zhang, Appl. Phys. Lett. **90**, 012904 (2007).
[36]F. Hong, Z. X. Cheng, S. J. Zhang, and X. L. Wang, J. Appl. Phys. **111**, 034104 (2012).